Palladium colloids from an organometallic route: redox reaction between $[VCp_2]$ and $[(Pd(\eta^3\text{-allyl})_2Cl]_2$. Catalytic application to the hydrogenation of aromatic nitro compounds

Jean-Louis Pellegatta,[a] Claudine Blandy,[a] Robert Choukroun,*[a] Christian Lorber,[a] Bruno Chaudret,[a] Pierre Lecante[b] and Etienne Snoeck[b]

[a] *Laboratoire de Chimie de Coordination du CNRS (UPR 8241) - 205, route de Narbonne, 31077, Toulouse Cedex 4, France*
[b] *CEMES-LOE-CNRS, 29 rue Jeanne Marvig, BP 4347, 31055, Toulouse Cedex, France*

Received (in Montpellier, France) 18th March 2003, Accepted 3rd July 2003
First published as an Advance Article on the web 2nd September 2003

$[Pd(\eta^3\text{-}C_3H_5)_2Cl]_2$ reacts in THF in the presence of poly(vinylpyrrolidone) (PVP), with the 15-electron complex vanadocene $[V(C_5H_5)_2]$, to give PVP-protected palladium particles. High resolution electron microscopy (HREM) and wide angle X-ray scattering (WAXS) experiments were carried out on the PVP-protected palladium particles as obtained when exposed to H_2 and O_2 and after hydrogenation catalysis. In each case, the particles display the fcc lattice of bulk palladium and a narrow size distribution centred near 2–3 nm. Catalytic hydrogenation reactions of nitrotoluene and 2,4-dinitrotoluene into their corresponding aniline and 2,4-diaminotoluene were performed in CH_2Cl_2 and in H_2O/CH_2Cl_2 biphasic conditions. The catalytic reactions were found to be zero order with respect to the substrate and first order with respect to dihydrogen and catalyst.

Introduction

The past decade has demonstrated the importance of the role of colloids in various catalytic reactions,[1] primarily for hydrogenation of arenes.[2] Different synthetic pathways are presently studied to obtain various types of colloids displaying a controlled size and chemical environment. The most popular method for the preparation of noble metal particles involve reduction of chloride precursors by various reducing agents, for example refluxing alcoholic solutions in the presence of a polymer.[3,4] In our group, the role of the vanadocene $[VCp_2]$ as an organometallic reducing agent to prepare metal colloids embedded in a PVP polymer matrix (PVP: polyvinylpyrrolidone) was successfully demonstrated in the case of $FeCl_2$ and more recently of $[Rh(C_2H_4)_2Cl]_2$, to give Fe and Rh nanoparticles.[5] This unusual synthetic organometallic route allows to prepare colloids using organometallic complexes containing chloride group(s). A small amount of residual chloride groups may be present on the metal surface and/or some trace of $[VClCp_2]$ could be included in the colloids–PVP material, as suggested by analytical results. Nevertheless, the magnetic or catalytic properties of the colloids are not affected and, very recently, Rh colloids were found to be active towards the hydrogenation of benzene, a test to demonstrate the presence of rhodium particles.[6] Colloidal palladium has been known for a long time and the use of palladium and other colloidal catalysts has recently attracted much attention in hydrogenation of nitro aromatics.[7,8] Pursuing our research on polymer-stabilized noble metal colloidal catalysts, we report in this paper the formation of palladium colloids *via* an organometallic route using $[VCp_2]$ as reducing agent and some kinetic results on the hydrogenation of the nitro group attached to an aryl ligand.

Results and discussion

Synthesis and characterization (HRTEM, WAXS) of palladium colloids

The reaction of a THF solution of $[Pd(\eta^3\text{-allyl})_2Cl]_2$ with 2 equiv. $[VCp_2]$ in the presence of polyvinylpyrrolidone (K30-PVP, average molecular weight: 40 000) as protecting polymer at room temperature leads to palladium colloids dispersed in PVP and isolated as the black solid [Pd-PVP] (Scheme 1). The product can be easily purified by washing several times with a mixture of THF/toluene to eliminate $[VClCp_2]$, and possibly unreacted $[VCp_2]$. The solid is soluble in alcoholic and chlorinated solvents as well as in water, but is insoluble in aliphatic and aromatic solvents. A low magnification TEM micrograph of the solid shows that the particles are well dispersed. The HREM micrograph in Fig. 1 evidences fringes in the particles. The regular periodicity of the fringes allows the determination of the fcc structure of the particles. The histogram in Fig. 2 shows a mean diameter for the particles of about 1.8 nm, with a relatively large size distribution. Structural characterization of the palladium colloids by wide angle X-ray scattering (WAXS) was performed in the solid state, on the same batch, using procedures previously validated for colloids in PVP.[9] This technique, in which the radial distribution function (RDF) gives a Pd–Pd distance of 2.75 Å confirms the fcc structure of the particles (Fig. 3, curve a). The coherence length can be evaluated to 2 nm, in agreement with TEM

$$2\,[VCp_2] + [Pd(\eta^3\text{–allyl})_2Cl]_2 \xrightarrow[\text{THF/ toluene}]{\text{PVP}} \text{"Pd"} + 2[VClCp_2] + (C_3H_6 + \ldots)$$

Scheme 1

 DOI: 10.1039/b303130f

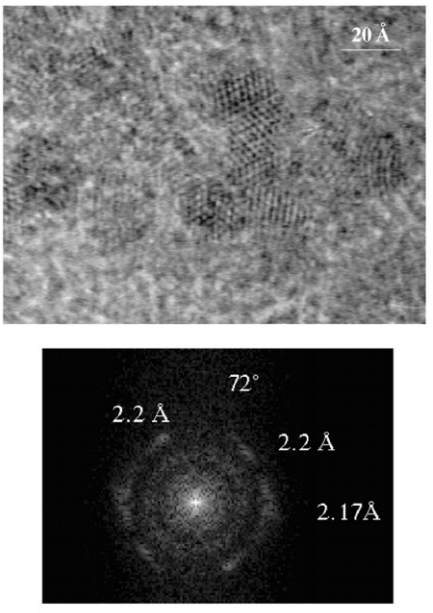

Fig. 1 HREM micrograph evidencing the fcc structure of palladium particles.

measurements. The same RDF was observed when solid [Pd–PVP] was treated with O_2 or CO (20 bar, 4 days). With O_2, the RDF gives direct evidence of the absence of significant oxidation of the sample, at least in the core of the nanoparticles (a slight oxidation on the surface of the colloids has been observed by EDAX techniques).[10] After exposure to H_2 of the colloids, the RDF curve is dramatically modified: the colloids still adopt the fcc structure with an unmodified Pd–Pd distance, but the coherence length now extends up to at least 3 nm, indicating larger and/or more crystalline nanoparticles (Fig. 3, curve b).

The concentration of palladium embedded in the polymer can be modulated as a function of the different amounts of PVP added (5% to 13% in Pd weight).

Hydrogenation of 2,4-dinitrotoluene with Pd colloids

The catalytic properties of these nanoparticles were investigated on the hydrogenation of nitro substituents attached to toluene as 2,4 dinitrotoluene (2,4-DNT). For each catalytic reaction described below, the same [Pd–PVP] catalyst batch was used (*i.e.* Pd = 13%). The solid was used as a soluble heterogeneous catalyst in CH_2Cl_2.

The hydrogenation of nitrobenzene into aniline was selected as a test reaction to demonstrate that i) the metal is in its active

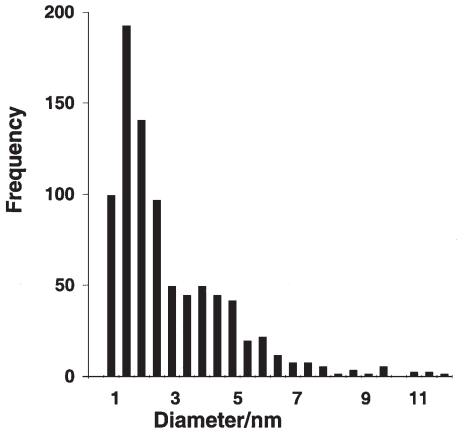

Fig. 2 Histogram of the Pd nanoparticle diameters.

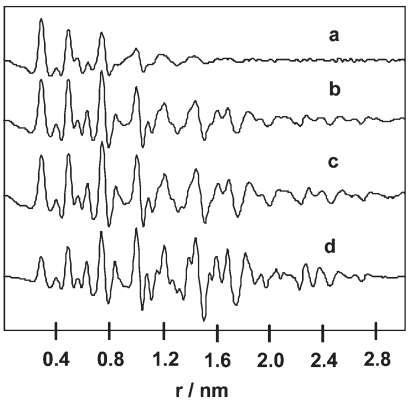

Fig. 3 WAXS RDF of (a) palladium particles, (b) palladium particles after exposure to H_2, (c) palladium particles after the first catalytic run, (d) simulation of a spheric 935-atom model.

form for the catalysis, ii) the experimental conditions *i.e.* the use of CH_2Cl_2 as chlorinated solvent is not a poison for the potential catalytic surface (as observed recently with a supported palladium complex[11]). The reaction was monitored by GC, using the following experimental conditions: [catalyst]/[substrate] ratio of 1/250, 10 mL CH_2Cl_2 ([substrate] 0.47 mol·L^{-1}), dodecane as internal standard, 40 °C under 7 bar H_2 and a stirring rate of 750 rpm (which was chosen to eliminate all consideration on interphase mass transfer). The linear plot of the nitrobenzene disappearance rate with time corresponds to an apparent rate of 31×10^3 mol·L^{-1}·h^{-1}·atom^{-1}. It is clear from this preliminary result that the hydrogenation of the nitro group occurs and that the liberated water (2 H_2O) formed in the reaction has not affected the course of the catalysis. The complete hydrogenation of the aromatic cycle *i.e.* the formation of cyclohexylamine was never observed.

To go further, different series of 2,4-DNT hydrogenation were carried out under the same experimental conditions, with the concentration of the substrate varying from 0.2 to 2 mol·L^{-1} (the solubility of solid 2,4-DNT in CH_2Cl_2 at 40 °C was measured by chromatography of a saturated solution and found to be 2.1 ± 0.1 mol·L^{-1}). The hydrogenation of 2,4-DNT into the corresponding 2,4-diaminotoluene (2,4-DAT) follows the formal reaction pathways described in Scheme 2 where r_1, r_2, r_3 are the hydrogenation rates of 2,4-DNT into respectively 4-amino-2-nitrotoluene (4A2NT), 2-amino-4-nitrotoluene (2A4NT) and 2,4-DAT; r'_1, r'_2 are the hydrogenation rates of 4A2NT and 2A4NT into 2,4-DAT. Fig. 4 shows a typical distribution of the hydrogenation products in the liquid phase as a function of time. It is clear that during the first half-part of the reaction (t = 2.5 h), while 2,4-DNT is still present, the orders with respect to all the products are

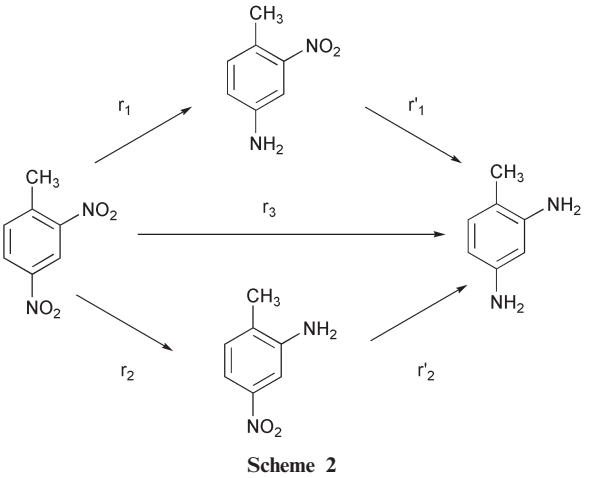

Scheme 2

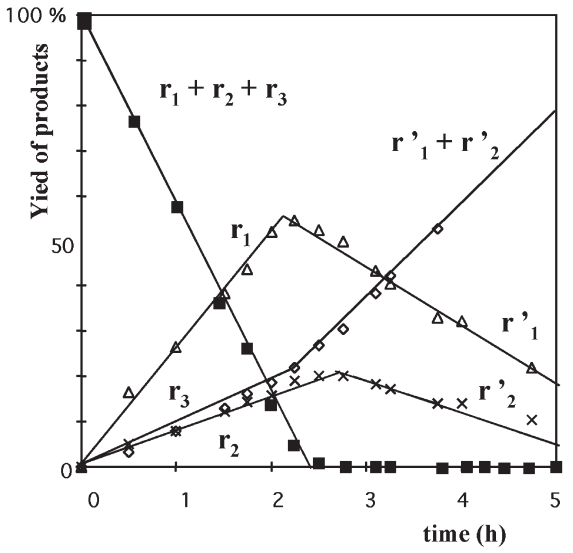

Fig. 4 Distribution products observed during the catalytic hydrogenation of 2,4-DNT (■: 2,4 dinitrotoluene (2,4-DNT); △: 4-amino, 2-nitro-toluene (4A2NT); ◇: 2,4-diamino-toluene (2,4-DAT); ×: 2-amino,4-nitro-toluene (2A4NT)).

zero (all the variations are linear). The final 2,4-DAT product is directly obtained in one step ($r'_1 + r'_2 = 0$). The maximal concentration of 4A2NT and 2A4NT is obtained when the reduction of 2,4-DNT is essentially complete (as viewed by the steep beak observed for the corresponding curves in Fig. 4). We note that reduction of 4A2NT and 2A4NT into 2,4-DAT depends on the concentration of 2,4-DNT still present in solution. There is a strong preference for catalyst-2,4-DNT bonding in such a manner that 2,4-dinitrotoluene has to be converted into monoamino intermediates before the transformation of the latter into 2,4-DAT. During the second half-part of the reaction, the zero orders are confirmed and the two monoamino intermediates are reduced to the final 2,4-DAT.

Additional experiments on 2,4-DNT hydrogenation were performed using different concentrations of the substrate for testing a possible influence on the rate of the reaction.

From the rate values obtained for 4 runs with different initial concentrations of 2,4-DNT (Table 1, Fig. 5), it can be seen that its hydrogenation into 4A2NT is faster than that of 2,4-DNT (d curve > g or e curve) *i.e.* $r_1 > r_2$ or r_3. It is interesting to note that the *p*-NO_2 substituent is hydrogenated before *o*-NO_2 on the catalytic surface, due to its better accessibility on the surface.[12] The hydrogenation rate of 4A2NT, is however still higher than that of 2A4NT, which has a *p*-NO_2 attached

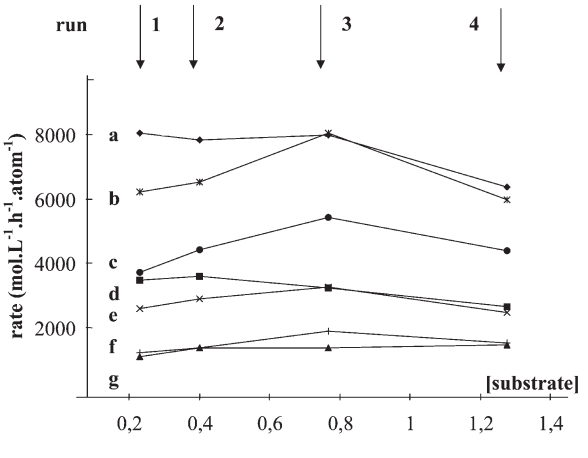

Fig. 5 Rate values of the distribution products obtained during the catalytic hydrogenation of 2,4-DNT at 4 different initial concentrations (a: $r_1+r_2+r_3$; b: $r'_1+r'_2$; c: r'_1; d: r_1; e: r_3; f: r'_2; g: r_2).

to the toluene ring (c curve > f curve so $r'_1 > r'_2$). This observation has already been pointed out[7b] and the better reactivity of the *ortho* position suggests that electronic effects are now preponderant over steric effects.

The hydrogenation of the intermediates 2A4NT and 4A2NT was also separately performed using a [catalyst]/[substrate] ratio of 1/250 and a substrate concentration of 0.23 mol L^{-1}. As expected, the hydrogenation rates r'_1 and r'_2 for 4A2NT and 2A4NT respectively are 3.04 and 1.13×10^3 mol·L^{-1}·h^{-1} $atom^{-1}$. These values are in the same order range as those obtained previously for the hydrogenation of 2,4-DNT as r'_1 and r'_2 (see Table 1, entry 1) and confirm that the hydrogenation rate of 4A2NT is roughly three times that of 2A4NT. We also verified that the disappearing rate of the substrate (Fig. 5, curve a) is roughly equal to the sum of the three values $r_1+r_2+r_3$ for each concentration. On the basis of this observation, it is clear that 2,4-DNT, 2A4NT and 4A2NT are simultaneously adsorbed on the nanoparticles. It is interesting to note that the hydrogenation rate per atom of Pd remains roughly constant (within experimental errors) whatever the concentration of the substrate, especially if we consider the results obtained for the higher and lower concentration values of Table 1 (entry 1 and 4).

On the other hand, 2-(hydroxyamino)-4-nitrotoluene (2H4ANT) and 4-(hydroxyamino)-2-nitrotoluene (4H2ANT) were previously identified as intermediates in the catalytic hydrogenation of 2,4 DNT over a Pd/C catalyst.[13] Following the experimental procedure of these authors, neither isomeric intermediate was observed in our GC analysis. Nevertheless, we cannot exclude the presence of these highly reactive intermediates in our catalytic system [besides (i) the disappearing rate of the substrate which is roughly equal to the sum of the three values $r_1+r_2+r_3$ for each concentration; (ii) the quantitative analysis, with dodecane as an internal standard which shows a positive mass balance indicating that all the products obtained are identified by GC analysis]. The catalytic hydrogenation reaction was also examined for catalyst concentration and pressure effects. A first order reaction with respect to the solid catalyst was confirmed by comparing the rate of disappearance of 2,4-DNT (3.74×10^3 mol·L^{-1} h^{-1} $atom^{-1}$ and 8.01×10^3 mol·L^{-1} h^{-1} $atom^{-1}$) for two different [catalyst]/[substrate] ratios (1/560 and 1/250) with the same substrate concentration (0.8 mol L^{-1}). A further experiment was carried out at 3.5 bar H_2 to identify the order with respect to dihydrogen for low pressures. We obtained, for a substrate concentration of 2 mol·L^{-1}, a complete hydrogenation in 2.25 h at 7 bar and in 4.5 h at 3.5 bar. These results indicate a first order reaction with respect to dihydrogen.

According to a model based on a Langmuir–Hinshelwood type of mechanism, the rate law can be written as $r = k'$ [catalyst][H_2], k' being the apparent constant taking into account all adsorption phenomena (calculations of k' as reported by Janssen and colleagues.[14] were not carried out since the surface of the solid is not uniform and contains different catalytic sites as edge, summit, surface).

Table 1 Hydrogenation rate values[a] of 2,4-DNT and their intermediate products at different concentrations (*r* being defined in Fig. 4 and in the text)

Run No.	[DNT]	$r_1+r_2+r_3$ (a)	r_1 (d)	r_2 (g)	r_3 (e)	$r'_1+r'_2$ (b)	r'_1 (c)	r'_2 (f)
1	0.229	8.10	3.53	1.16	2.63	6.27	3.78	1.27
2	0.400	7.88	3.66	1.42	2.96	6.57	4.48	1.42
3	0.768	8.01	3.28	1.43	3.30	8.09	5.46	1.95
4	1.276	6.40	2.72	1.51	2.53	6.02	4.45	1.57

[a] $r\ 10^{-3}$ (mol L^{-1} h^{-1} $atom^{-1}$)

Hydrogenation of 2,4-dinitrotoluene in biphasic conditions (H_2O/CH_2Cl_2)

The catalyst was also used as a soluble heterogeneous solid in biphasic conditions (CH_2Cl_2/water). The [Pd–PVP] is dissolved in 3 ml H_2O and the substrate dissolved in 10 ml of CH_2Cl_2 is added. It is noteworthy that the CH_2Cl_2 phase remains colorless and hence that no catalyst is transferred into the organic phase (*vide intra*). The hydrogenation was carried out in our standard experimental conditions ([catalyst][substrate] ratio 1/250; 40 °C, 7 bar H_2, stirring rate 750 rpm, dodecane as internal standard) and the rate of the disappearance of 2,4-DNT was found to 32.2 $mol{\cdot}h^{-1}{\cdot}atom^{-1}$. The catalyst is easily separated by decanting and the aqueous phase reused for a second biphasic hydrogenation cycle. The rate of the disappearance of 2,4-DNT was found to increase after the second catalytic cycle (two cycles) from 32.2 to 46.4 $mol{\cdot}h^{-1}{\cdot}atom^{-1}$ probably because of a slight evolution of the microstructure of the solid (*vide infra*). On the other hand, the organic CH_2Cl_2 phase was reused with the same quantity of 2,4-DNT and H_2O and no catalytic activity was observed. This fact confirms that the catalyst is maintained in the aqueous phase.

Characterization of the re-used catalyst in the biphasic hydrogenation

The aqueous phase from the reaction described above was then recuperated and after complete elimination of water *in vacuo*, the catalyst was recovered and analyzed by WAXS technique (Fig. 3, curve c) which shows the RDF curve obtained for Pd nanoparticles after the first catalytic run. The RDF curve is still well resolved and does not indicate any reduction in size or crystallinity of the nanoparticles. TEM observation of the particles before catalysis (dissolved in methanol and treated with H_2) and after catalysis shows well dispersed nanoparticles (Fig. 6) with a narrow size distribution centred near 2–3 nm (Fig. 7), in contrast to the size distribution observed on the crude Pd–PVP, directly obtained from synthesis. The role of H_2 on the colloids was already pointed out[10] and we recently observed the influence of H_2 on rhodium particles.[5b] The treatment of a heterogeneous solution of Pd colloids with H_2 clearly leads to a lower size distribution of the particles with a higher crystallinity and, as a consequence, can increase the number of atoms accessible to the catalysis on the surface of the colloids. A simulated reduced intensity function can be computed using Debye's formula applied to a theoretical proposed model consistent in size and structure, in this case with a spheric 935-atom model. A Fourier transform of this function then provides a simulated RDF (Fig. 3, curve d) which can be fitted well to the experimental one (Fig. 3, curves b or c). The agreement is good enough to confirm the fcc lattice inside the particles: all distances generated by the model match peaks in the RDF (a large cluster of 923 atoms, *i.e.* 6-shell Pd nanoparticles, gives a theoretical diameter of 2.87 Å).

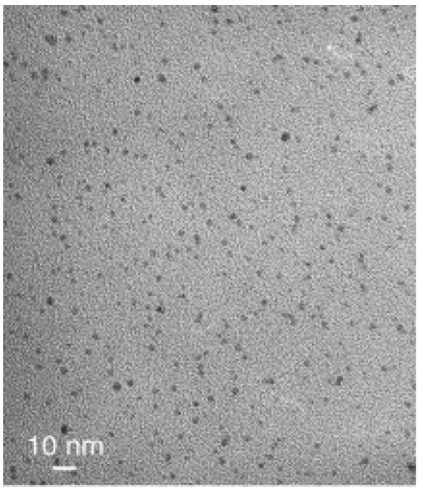

Fig. 6 TEM of the Pd nanoparticles after catalysis.

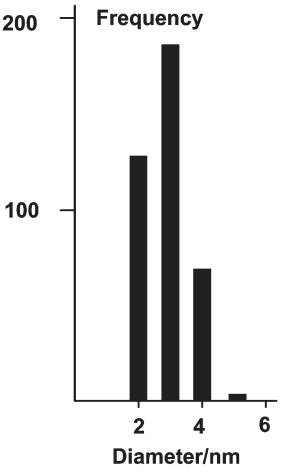

Fig. 7 Histogram of the Pd nanoparticle diameters after catalysis.

Conclusion

Palladium particles were synthesized following an organometallic route, from a chloro-palladium(I) complex. Investigations by TEM and Wide Angle X-ray Scattering (WAXS) evidence the higher degree of crystallinity of the fcc palladium particles when the colloids are treated with H_2 in solution. The average size of the particles is then affected and a more narrow size distribution is observed after hydrogen treatment. Hydrogenation of nitroaromatics to anilines is demonstrated in chlorinated solvent and in biphasic H_2O/CH_2Cl_2 conditions. Under the latter experimental conditions, all the nanoparticles are concentrated in the aqueous phase. Kinetic studies show the reactions to be zero order with respect to the substrate and first order with respect to hydrogen and catalyst. Hydrogenation of halonitroaromatics to their corresponding haloaniline, is currently in progress.

Experimental

Syntheses and analysis

The synthesis of the palladium particles was carried out under an inert Ar atmosphere in a glove box, typically as follows: a mother solution of 800 mg of PVP in 20 mL of THF was divided in nearly two equal volumes and added to a THF solution (5 mL) of 150 mg of [VCp_2] (0.83 mmol) and to a THF (5 mL) solution of 140 mg of [$Pd(\eta^3\text{-allyl})_2Cl]_2$ (0.83 mmol). Under vigorous stirring, the Cp_2V solution was added dropwise to the palladium solution. The resulting solution turned black and stirring was continued for 12 hours during which time the colloids precipitated. The solution was concentrated to 5 mL and 15 mL of toluene were added. The resulting black solid PVP-protected palladium colloid was filtered and washed thoroughly (10 mL Toluene/THF 3 : 1, 3 × 10 mL toluene/THF 2 : 1, and 10 mL toluene/THF 1 : 1). The black solid thus obtained was finally dried (500 mg, elem. anal.: Pd = 13%, V = 0.52%, Cl = 0.29%). After work-up of the THF/toluene filtrate of the solution, [$VClCp_2$] was fully characterized by C, H elemental analysis and ^1H NMR. An analogous experiment in a closed vessel was also performed. The gas phase analysed by MS and IR shows the presence of propene, probably resulting from the combination of the allyl moiety with a hydrogen atom of the THF solvent.[15]

Electron microscopy

TEM samples were prepared by slow evaporation in the glove box of one drop of a diluted solution of the product in methanol deposited on a carbon coated copper grid. Reproducible HREM images were obtained on samples produced from independent syntheses. The experiments were performed on a Philips CM 30/ST operated at 300 kV with point resolution 0.19 nm. The size distribution was measured through the numerical analysis of TEM low magnification images. In this procedure, the different particles were first identified according to an upper and lower intensity threshold, then counted and measured. HRTEM images of isolated particles were digitized at a resolution of 0.03 nm pix^{-1} and analysed using their numerical diffractograms (Fourier transforms). Transmission electron microscopy (TEM) of the particles in MeOH solution under H_2 and after catalysis was performed on a JEM 2010 operating at an accelerating voltage of 200 kV with point resolution 0.23 nm. Samples were prepared in a glove box under argon and were examined at magnification between 100 and 400 K. For each sample, and due to the small size of the particles, the diameters of a large number (nearly 400) of Pd particles were determined from enlarged photoimages in order to obtain a size distribution with good statistics.

WAXS experiments

Solid samples for WAXS experiments were introduced in thin walled Lindemann capillaries of 1.5 mm diameter, in a glove box filled with argon; the capillaries were sealed for the experiments. Measurements were carried out as previously described.[9] Data were normalized to one palladium atom. Reproducible WAXS patterns were obtained on samples produced from independent syntheses.

Catalysis experiments

Hydrogen C grade was supplied by Air Liquide. Gas chromatography mass spectrometry (GC-MS) was performed using a Nermarg R10-10 with a ionizing voltage of 70 eV. The catalytic reactions were carried out in a 250 ml Fisher–Porter bottle connected to the H_2 tank and maintained at 40 °C in an oil bath.

The small size of the particles excludes the presence of internal mass transfer limitations. The first order with respect to the catalyst confirms the absence of external mass transfer limitations.

The [catalyst]/[substrate] ratio was calculated according to the concentration of palladium atoms contained in the [Pd–PVP] catalyst. In a typical experiment, colloids (15 mg, 13% wt) and H_2O (5 ml) were stirred at 750 rpm during 15 min until complete dissolution of the catalyst took place. A solution of 2,4-DNT (0.362 g, 2.96 mmol) in 10 ml CH_2Cl_2 was then added and the gas admitted (7 bar). Samples of the organic phase were removed from time to time for GC analyses.

Acknowledgements

We thank V. Collière for his technical assistance.

References

1 (*a*) G. Schmid, in *Clusters and Colloids*, VCH, Weinheim, 1994; (*b*) G. Schmid, V. Maihack, F. Lantermann and S. Peschel, *J. Chem. Soc., Dalton Trans.*, 1996, **5**(1), 589; (*c*) H. Hirai, *J. Macromol. Sci. Chem.*, 1979, **A13**, 633; (*d*) H. Bönnemann and W. Brijoux, in *Active Metals*, ed. A. Fürnstner, VCH, Weinheim, 1996, p. 339–376; (*e*) H. Bönnemann, G. Braun, W. Brijoux, R. Brinkmann, A. Schulze Tilling, K. Seevogel and K. Siepen, *J. Organomet. Chem.*, 1996, **520**, 143; (*f*) H. Bönnemann, W. Brijoux, R. Brinkmann and E. Dinjus, *J. Mol. Catal.*, 1992, **74**, 323; (*g*) J. D. Aiken III and R. G. Finke, *J. Mol. Catal.*, 1999, **145**, 1; (*h*) J. D. Aiken III and G. Finke, *J. Chem. Soc.*, 1998, **120**, 9545; (*i*) J. D. Aiken III and R. G. Finke, *J. Am. Chem. Soc.*, 1999, **121**, 8803; (*j*) J. Schulz, A. Roucoux and H. Patin, *J. Chem. Soc., Chem. Commun.*, 1999, 535; (*k*) C. Larpent, E. Bernard, F. Brisse-Le Menn and H. Patin, *J. Mol. Catal.*, 1997, **116**, 277; (*l*) J. Dupont, G. S. Fonseca, A. P. Umpieree, P. F. P. Fichtner and S. R. Texeira, *J. Am. Chem. Soc.*, 2002, **124**, 4228; (*m*) A. Roucoux, J. Schulz and H. Patin, *Chem. Rev.*, 2002, **102**, 3257.

2 J. A. Widegren and R. G. Finke, *J. Mol. Catal. A*, 2003, **191**, 187 and references therein.

3 (*a*) *Advances in catalysis and nanostructured materials*, ed. W. R. Moser, Academic Press, 1966; (*b*) H. Hirai and N. Toshima in *Catalysis by metal complexes, Tailored metal catalysts*, ed. Y. Iwasawa, D. Reidel Publishing Company, Dordrecht, 1986; (*c*) J. S. Bradley, in *Clusters and Colloids. From theory to applications*, ed. G. Schmid, VCH, Weinheim, 1994; (*d*) M. N. Vargaftik, V. P. Zagorodnikov, I. P. Stolarov, I. I. Moiseev, D. I. Kochubey, V. A. Likholobov, A. L. Chuvilin and K. I. Zamaraev, *J. Mol. Catal.*, 1989, **53**, 315; (*e*) N. A. Dhas and A. Gedanken, *J. Mater. Chem.*, 1998, **8**, 445; (*f*) N. A. Dhas, H. Cohen and A. Gedanken, *J. Phys. Chem. B*, 1997, **101**, 6834; (*g*) F. Dassenoy, K. Philippot, T. Ould Ely, C. Amiens, P. Lecante, E. Snoeck, A. Mosset, M.-J. Casanove and B. Chaudret, *New. J. Chem.*, 1998, **22**, 703; (*h*) C. Pan, F. Dassenoy, M.-J. Casanove, K. Philippot, C. Amiens, P. Lecante, A. Mosset and B. Chaudret, *J. Phys. Chem. B*, 1999, **103**, 10 098; (*i*) S. Gomez, L. Erades, K. Philippot, B. Chaudret, V. Collière, O. Balmes and J.-O. Bovin, *Chem. Commun.*, 2001, 1474; (*j*) F. Dumestre, B. Chaudret, C. Amiens, M.-C. Fromen, M.-J. Casanove, P. Renaud and P. Zurcher, *Angew. Chem. Int. Ed.*, 2002, **41**, 4286; (*k*) K. Pelzer, O. Vidoni, K. Philippot, B. Chaudret and V. Collière, *Adv. Funct. Mater.*, 2003, **13**, 118.

4 (*a*) M. T. Reetz, M. Winter and B. Tesche, *Chem. Mater.*, 1998, **10**, 147; (*b*) H. Bönnemann, W. Brijoux, K. Siepen, J. Hormes, R. Franke, J. Pollmann and J. Rothe, *Appl. Organomet. Chem.*, 1997, **11**, 783; (*c*) S. Y. Troitski, M. A. Serebriakova, M. A. Fedotov, S. V. Ignashin, A. L. Chuvilin, E. M. Moroz, B. N. Novgorodov, D. I. Kochubey, V. A. Likholobov, B. Blanc and P. Gallezot, *J. Mol. Catal. A*, 2000, **158**, 461; (*d*) H. Bönnemann and W. Brijoux, in *Advanced Catalysts and Nanostructured Materials*, ed. W. R. Moser, Academic Press, 1996, 65; (*e*) A. B. R. Mayer and J. E. Mark, in ACS Symposium Series, Nanotechnology, 1996, No. 622, Chapter 9, 137–150.

5 (*a*) R. Choukroun, D. de Caro, S. Matéo, C. Amiens, B. Chaudret, E. Snoeck and R. Respaud, *New J. Chem.*, 1998, **22**, 1295; (*b*) R. Choukroun, D. de Caro, B. Chaudret, P. Lecante and E. Snoeck, *New J. Chem.*, 2001, **25**, 525.

6 J.-P. Pellegatta, C. Blandy, V. Collière, R. Choukroun, B. Chaudret, P. Cheng and K. Phillippot, *J. Mol. Catal. A*, 2002, **178**, 55.

7 (*a*) B. Amon, H. Redlingshöfer, E. Klemm, E. Dieterich and G. Emig, *Chem. Eng. Process.*, 1999, **38**, 395; (*b*) G. Neri, M. G. Musolino, C. Milone, D. Pietropaolo and S. Galvagno, *Appl. Catal. A*, 2001, **208**, 307.

8 (*a*) Z. Yu, S. Liao, Y. Xu, B. Yang and D. Yu, *J. Mol. Catal. A*, 1997, **120**, 247; (*b*) X. Yan, M. Liu, H. Liu and K. Y. Liew, *J. Mol. Catal. A*, 2001, **169**, 225; (*c*) X. Yan, M. Liu, H. Liu, K. Y. Liew and N. Zhao, *J. Mol. Catal. A*, 2001, **170**, 203; (*d*) W. Tu, H. Liu and Y. Tang, *J. Mol. Catal. A*, 2000, **159**, 115; (*e*) B. Coq, A. Tijani, R. Dutartre and F. Figuéras, *J. Mol. Catal.*, 1993, **79**, 253; (*f*) W. Yu, M. Liu, H. Liu, X. An, Z. Liu and X. Ma, *J. Mol. Catal. A*, 1999, **142**, 201.

9 M. Bardaji, O. Vidoni, A. Rodriguez, C. Amiens, B. Chaudret, M. J. Cazanove and P. Lecante, *New J. Chem.*, 1997, **21**, 1243.

10 T. Teranihi and M. Miyake, *Chem. Mater.*, 1998, **10**, 594.

11 M. M. Del Anna, M. Gagliardi, P. Mazstrorilli, G. P. Suranna and C. F. Nobile, *J. Mol. Catal. A*, 2000, **158**, 515.

12 M. G. Musolino, C. Milone and G. Neri, *Heterogeneous Catalysis and Fine Chemicals IV*, eds. H. U. Blaser, A.Baiker and R. Prins, Elsevier Science B.V, 1997.

13 G. Neri, M. G. Musolino, E. Rotondo and S. Galvagno, *J. Mol. Catal.*, 1996, **111**, 257.

14 H. J. Janssen, A. J. Kruithof, G. J. Steghuis and K. R. Westerperp, *Ind. Eng. Chem. Res.*, 1990, **29**, 1822.

15 P. M. Maitlis, *The organic Chemistry of Palladium*, eds. P. M. Maitlis, F. G. A. Stone and R. West, Academic Press, N.Y., 1971, vol. 1.